JOURNAL OF GUIDANCE, CONTROL, AND DYNAMICS
Vol. 20, No. 5, September–October 1997

Analysis of the Frequency, Damping, and Total Insensitivities of Input Shaping Designs

Lucy Y. Pao
University of Colorado, Boulder, Colorado 80309-0425

In the modeling of flexible structures, there is generally uncertainty in both the frequencies and damping constants, and, thus, it is important that the control methods for such systems be robust to these uncertainties. Input shapers have been shown to yield good performance while being insensitive to modeling errors. Most previous studies, however, have addressed only frequency modeling errors. In this study, modeling errors in damping are considered as well, and a total insensitivity measure is defined that incorporates both frequency and damping modeling errors. An analysis of several types of input shapers shows a different ordering of shaper types in terms of their total insensitivity to frequency and damping modeling errors compared to previous studies and comparisons of these shaper types in terms of uncertainty in frequency alone.

I. Introduction

ACCURATE control of flexible structures is an important and difficult problem and has been an active area of research.[1,2] Methods that have been investigated for controlling flexible structures can be roughly divided into feedback and feedforward approaches. Feedback control methods use measurements and estimates of the system states to reduce vibration, whereas feedforward techniques alter the actuator commands or setpoints so that system oscillations are reduced (see Fig. 1). Feedback methods alone are generally computationally complex and, hence, are not very practical for real-time implementation. The performance of feedback methods can often be improved by additionally using a feedforward controller, and properly designed feedforward compensators can dramatically reduce the complexity of the required feedback controllers for a given level of performance.

One feedforward method, known as input shaping, has been successfully applied for controlling flexible structures, and the technique has been shown to allow flexible structures to be maneuvered with little residual vibration, even in the presence of modeling uncertainties and structural nonlinearities.[3–6] In this method, an input command is convolved with a sequence of impulses designed to produce a resulting input command that causes less residual vibration than the original unshaped command (see Fig. 1). The goal of input shaping is to determine the amplitudes and timing of the impulses to eliminate or reduce residual vibration. Because only the timing and amplitudes need to be stored and only convolution needs to be performed in real time, input shapers are a very practical method of reducing vibrations.

The effectiveness of input shaping has been demonstrated on many types of systems. It was used to improve the throughput of a wafer handling robot[7] and the repeatability of a coordinate measuring machine.[8] Input shaping was a major component of a flexible system control experiment on the Space Shuttle Endeavor in March 1995 (Ref. 9), and it has also been investigated as a means of reducing residual vibrations of long-reach manipulators[10,11] for handling hazardous waste.

How sensitive input shapers are to modeling errors has been primarily addressed in terms of modeling errors in frequency only. However, damping is often more uncertain and difficult to model. In this paper, we develop the concept of damping insensitivity and a definition of total insensitivity that includes both frequency and damping modeling uncertainty, and we use these measures to analyze several types of input shapers. The shapes of the sensitivity contours in the ζ–ω space of various shapers are discussed, and a method for determining whether a common form of frequency and damping uncertainty can be accommodated by various shaper types is presented.

The paper is organized as follows. In Sec. II, we briefly review input shaping and show how some shapers that have been developed for extra insensitivity to frequency modeling errors are not robust to damping uncertainty relative to other types of shapers. We define the concept of total insensitivity in Sec. III, and we analyze several types of input shapers using this measure. The sensitivity contour shapes of various input shapers are discussed in more detail in Sec. IV. Finally, concluding remarks are given in Sec. V.

II. Input Shaping Methods

We consider point-to-point control of flexible structures

$$\dot{\boldsymbol{x}}(t) = \boldsymbol{A}\boldsymbol{x}(t) + \boldsymbol{b}u(t) \tag{1}$$

where

$$\boldsymbol{A} = \text{blockdiag}[\boldsymbol{A}_j] = \text{blockdiag}\begin{bmatrix} 0 & 1 \\ -\omega_j^2 & -2\zeta_j\omega_j \end{bmatrix}$$

$$\boldsymbol{b} = [0 \quad b_0 \quad 0 \quad b_1 \quad \cdots \quad 0 \quad b_n]^T$$

Lucy Y. Pao received her B.S., M.S., and Ph.D. degrees in Electrical Engineering from Stanford University in 1987, 1988, and 1991, respectively. From 1991 to 1993, she worked at the MITRE Corporation, and from 1993 to 1995, she was an Assistant Professor in the Electrical Engineering and Computer Science Department at Northwestern University. Since 1995, she has been an Assistant Professor in the Electrical and Computer Engineering Department at the University of Colorado at Boulder. Pao is the recipient of the 1996 IFAC World Congress Young Author Prize, a National Science Foundation Early Faculty CAREER Development Award (1996–2000), and an Office of Naval Research Young Investigator Award (1997–2000). She has served on the IEEE Control Systems Society Conference Editorial Board (1995–1997), on the program committees of the American Control Conference (1995 and 1997), and as the American Automatic Control Council newsletter editor (1995–present). Her research interests are in the control of flexible structures, multisensor data fusion, human–machine and haptic interfaces, and dextrous robotics. She is a Member of AIAA.

Received June 10, 1996; presented as Paper 96-3844 at the AIAA Guidance, Navigation, and Control Conference, San Diego, CA, July 29–31, 1996; revision received May 7, 1997; accepted for publication May 11, 1997.

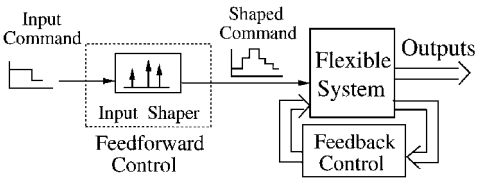

Fig. 1 Block diagram of combined feedforward/feedback control of a flexible system, where the feedforward compensator is an input shaper.

represent the flexible dynamics of the system; $\omega_1 < \cdots < \omega_n$ are the structural frequencies; and ζ_j, $j = 1, \ldots, n$, are the damping ratios of the flexible modes. Here, $\omega_0 = \zeta_0 = 0$ represents the rigid body mode of the structure. The state is defined as $\boldsymbol{x} = [x_1 \;\; x_2 \;\; x_3^1 \;\; x_4^1 \;\; \cdots \;\; x_3^n \;\; x_4^n]^T$, where x_1 and x_2 are the rigid body position and velocity and x_3^j and x_4^j are the modal positions and velocities. Desirable qualities of the control $u(t)$ are that it causes the motion to be performed rapidly while being robust to modeling errors.

The amplitudes and time locations of the impulses in an input shaper are determined by solving a set of nonlinear constraint equations. To limit the amount of residual vibration that occurs when the system reaches its desired setpoint, the vibration amplitude resulting from a sequence of impulses (the input shaper) is required to be less than a particular level at the final impulse time t_m. The residual vibration resulting from a sequence of impulses can be expressed as[3]

$$V(\omega, \zeta) = e^{-\zeta\omega t_m}\left[\left(\sum_{i=1}^{m} A_i e^{\zeta\omega t_i}\cos(\omega_d t_i)\right)^2 + \left(\sum_{i=1}^{m} A_i e^{\zeta\omega t_i}\sin(\omega_d t_i)\right)^2\right]^{\frac{1}{2}} \tag{2}$$

where $\omega_d = \omega\sqrt{(1-\zeta^2)}$; there are m impulses denoted by $i = 1, \ldots, m$; A_i is the amplitude of the ith impulse; and t_i is the time location of the ith impulse.

Various types of input shapers have been proposed for the control of flexible structures as in Eq. (1), including the following.

1) Zero vibration (ZV): Requiring that the flexible modal positions and velocities, x_3^j and x_4^j, $j = 1, 2, \ldots, n$, be zero after the sequence of impulses gives a set of ZV constraints.[3] This amounts to requiring that $V(\omega_j, \zeta_j) = 0$, $j = 1, 2, \ldots, n$.

2) Derivatives of ZV (ZVD): To increase the robustness of the impulse shaping sequence to modeling errors in the natural frequencies and damping ratios, the partial derivatives of the ZV constraints with respect to ω_j and ζ_j are also constrained to zero. These derivative constraints do not necessarily have to be imposed for all flexible modes, only those where extra robustness is desired.[3]

3) Additional derivatives of ZV (ZVDD, ZVDDD, etc.): Additional derivatives of various modes can be constrained to zero to further increase the insensitivity to modeling errors at those modes.[3]

4) Extra insensitive (EI): Another method of increasing robustness to modeling errors in the structural frequencies is to allow some finite residual vibration at the modeled frequency values but to constrain zero residual vibration at frequencies slightly above and below the modeling frequencies.[5] This amounts to requiring that $V(\omega_{\mathrm{lo}_j}, \zeta_j) = V(\omega_{\mathrm{hi}_j}, \zeta_j) = 0$, $j = 1, 2, \ldots, n$, where $\omega_{\mathrm{lo}_j} \le \omega_j \le \omega_{\mathrm{hi}_j}$. This EI method has the effect of broadening the frequency sensitivity curve about each modeling frequency and, hence, increasing the frequency insensitivity (see Fig. 2).

5) Two-hump EI, three-Hump EI, etc.: Additional robustness to uncertainty in structural frequencies can be obtained by requiring more than one hump in the frequency sensitivity curve[12,13] (Fig. 2). More and more robustness to frequency uncertainty is obtained by requiring $V(\omega, \zeta) = 0$ at more and more frequencies about the modeling frequencies.

Constraints to account for actuator limits are also included. Further requiring the impulses to be positive allows the shaper to be used with any arbitrary unshaped command input without violating the actuator limits if the original unshaped command does not violate

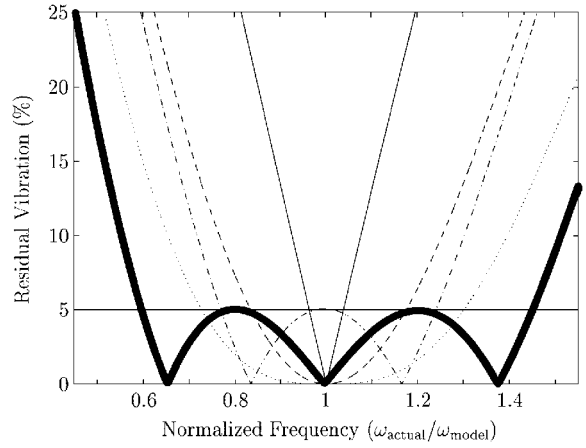

Fig. 2 Sensitivity curves relative to normalized frequency for various input shapers for a one-mode system: ——, ZV; - - - -, ZVD; · · · · ·, ZVDD; – · –, EI; and ▬▬, two-hump EI.

them.[3] However, if something is known about the types of unshaped commands that are used, shapers containing negative impulses can be designed to significantly reduce move time without overcurrenting the motors.[12,14,15] Sometimes the control inputs can only take on a small set of values,[4,12,14–16] such as in spacecraft with only on–off jets. Thus, there are several designs for each type of shaper (ZV, ZVD, EI, etc.).

Although many impulse sequences can satisfy a given set of these nonlinear constraints, because input shaping introduces a time lag (equal to the length of the impulse shaping sequence) into the actuator commands, the desired solution is the shortest impulse sequence satisfying the constraints. Input shaping has also been explored in the frequency domain, and it has been shown that control inputs causing little or no vibrations can be designed by ensuring that the transfer function of the control input has zeros at or near the locations of the poles of the flexible system.[17–20]

Figure 2 displays sensitivity curves relative to normalized frequency for typical ZV, ZVD, ZVDD, EI, and two-hump EI shapers for a one-mode [$n = 1$ in Eq. (1)] system. The plots are of Eq. (2) for a range of normalized frequencies $\omega/\omega_{\mathrm{model}} = \omega_{\mathrm{actual}}/\omega_{\mathrm{model}}$ with $\zeta = \zeta_{\mathrm{actual}} = \zeta_{\mathrm{model}}$. The residual vibration (2) using the ZV shaper is 0, where the actual system frequency is equal to the modeling frequency, i.e., there is no modeling error and $\omega_{\mathrm{actual}}/\omega_{\mathrm{model}} = 1$. As ω_{actual} deviates from ω_{model}, however, we see that the residual vibration increases rapidly. The other curves in Fig. 2 can be analyzed similarly.

Definition 1: Frequency insensitivity is the width I_f of the sensitivity curve relative to normalized frequency at a level V_a (such as 5%) of acceptable vibration.[3,5]

From Fig. 2, it is clear that the two-hump EI is more insensitive, i.e., has a greater 5% frequency insensitivity I_f, than the EI method. Similarly, the ZVDD is more insensitive than the ZVD, which is more insensitive than the ZV technique. The gains in insensitivity of the ZVD and EI over the ZV come at a cost in speed, that is, the ZVD and EI shapers lead to slower maneuvers, similarly for the increased insensitivity of the ZVDD and two-hump EI. The tradeoffs in speed vs insensitivity of several shaper designs have been investigated in Refs. 14 and 16.

The EI and multihump EI methods have generally been deemed superior to the ZVD and multiderivative approaches, with studies showing that, for comparable maneuver times, the EI methods lead to greater frequency insensitivity levels.[5,12,13] For instance, the EI and ZVD shapers lead to approximately the same move times, but the EI is less sensitive to modeling errors in frequency, as indicated by the broader frequency sensitivity curve for the EI compared to the ZVD in Fig. 2. Similarly, the two-hump EI has been shown to yield roughly the same maneuver times as the ZVDD but with greater insensitivity to frequency modeling errors, as again indicated by the broader frequency sensitivity curve for the two-hump EI compared with the ZVDD in Fig. 2.

However, the EI methods are only insensitive to frequency errors, whereas the ZVD and multiderivative methods are robust to

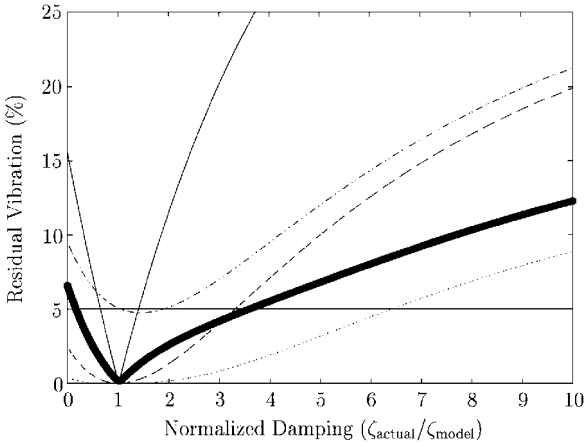

Fig. 3 Sensitivity curves relative to normalized damping ratio for various input shapers for a one-mode system: ——, ZV; - - - -, ZVD; · · · · ·, ZVDD; – · · –, EI; and ▬▬, two-hump EI.

uncertainty in both structural frequency and damping. Figure 3 shows sensitivity curves relative to normalized damping for the same ZV, ZVD, ZVDD, EI, and two-hump EI input shapers as in Fig. 2. The plots are of Eq. (2) for a range of normalized dampings $\zeta/\zeta_{model} = \zeta_{actual}/\zeta_{model}$ with $\omega = \omega_{actual} = \omega_{model}$.

Definition 2: Damping insensitivity is the width I_d of the sensitivity curve relative to normalized damping at a level V_a of acceptable vibration.

plane, this area can be thought of as a region about the modeled flexible poles of the system.

As mentioned in the preceding section, depending on actuator limit constraints and knowledge of the unshaped commands, there are several designs for each type (ZV, ZVD, EI, etc.) of shaper. Here, we consider the more general positive impulse shapers (shapers with only positive impulses) that can be used to shape arbitrary input commands without causing actuator saturation if the unshaped commands do not cause actuator saturation. For one-mode flexible systems, analytical or curve fit formulas exist for the amplitudes and timings of the impulses for the positive ZV, ZVD, ZVDD,[3] EI,[5] and two-hump EI[13] shapers. Two properties of these shapers simplify our analysis.

1) The amplitude formulas are only functions of the modeled damping constant ζ_{model}.

2) The time locations of the impulses in all cases are

$$t_i = \frac{\pi(i-1)}{\omega_{model}\sqrt{1-\zeta_{model}^2}} \tag{3}$$

The impulse amplitudes for some other shaper designs also have these properties.[14]

Because of these properties, the frequency, damping, and total insensitivity measures are constant as we vary ω_{model} while holding the modeled damping ζ_{model} constant. This can easily be verified by rewriting Eq. (2) for positive impulse single-mode shapers. Inasmuch as the impulse amplitudes and times, A_i and t_i, are functions of ζ_{model} and ω_{model}, the dependence of $V(\cdot)$ on them is explicitly indicated:

$$V(\omega, \zeta, \omega_{model}, \zeta_{model}) = \exp[-\zeta\omega_{norm}\pi(m-1)Z]$$
$$\times \left(\left\{ \sum_{i=1}^{m} A_i \exp[\zeta\omega_{norm}\pi(i-1)Z] \cos[\omega_{norm}\pi(i-1)Z_{norm}] \right\}^2 + \left\{ \sum_{i=1}^{m} A_i \exp[\zeta\omega_{norm}\pi(i-1)Z] \sin[\omega_{norm}\pi(i-1)Z_{norm}] \right\}^2 \right)^{\frac{1}{2}} \tag{4}$$

From Fig. 3, note that the EI is more sensitive to modeling errors in damping compared to the ZVD method. Similarly, the two-hump EI is more sensitive than the ZVDD to uncertainty in damping.

In virtually all previous studies, only the frequency insensitivity was considered; in fact, it was referred to as *the* insensitivity, and there were rare references to damping insensitivity. However, in practice, damping is often more uncertain and more difficult to model than structural frequency. For example, in lightly damped flexible systems, it is not uncommon to only know that the damping is in the range $0.01 < \zeta < 0.1$, where if the modeled damping is taken to be $\zeta_{model} = 0.01$, the actual damping ζ_{actual} could be as much as 10 times the modeled value. Further, damping can sometimes vary greatly during the operation of a system. For instance, in flexible systems where viscous coatings are used to increase damping, the coating properties can change dramatically with temperature variations, consequently causing the damping to also vary significantly.

III. Analysis of Total Insensitivity

Based on the discussion in the preceding section, it would be appropriate to develop a more complete definition of insensitivity than the individual frequency and damping insensitivities. In this section, we shall use the following measure to analyze and compare ZV, ZVD, ZVDD, EI, and two-hump EI shaper types for single-mode flexible systems.

Definition 3: Total insensitivity is the area I_{fd} in normalized ζ–ω space about the modeled damping and frequency such that the sensitivity surface lies below an acceptable vibration level V_a.

Equation (2) is evaluated for a range of normalized frequencies and dampings, $\omega/\omega_{model} = \omega_{actual}/\omega_{model}$ and $\zeta/\zeta_{model} = \zeta_{actual}/\zeta_{model}$, defining a surface in normalized ζ–ω space. The area of the region of ζ–ω space where the surface lies below the acceptable vibration level V_a is computed as the total insensitivity. In the s

where $\omega_{norm} = \omega/\omega_{model} = \omega_{actual}/\omega_{model}$ is the normalized frequency, $Z = 1/\sqrt{(1-\zeta_{model}^2)}$, and $Z_{norm} = \sqrt{(1-\zeta^2)}/\sqrt{(1-\zeta_{model}^2)}$.

For a given ζ_{model}, $V(\cdot)$ is only a function of the normalized frequency ω_{norm} and damping ζ. Thus, the sensitivity surface in normalized ζ–ω space will be the same regardless of ω_{model}, and, hence, the total insensitivity is independent of ω_{model}. Because the sensitivity surface is constant for different ω_{model}, the two cross sections of the surface at ζ_{norm} and $\omega_{norm} = 1$ are also invariant with ω_{model}. These cross sections are just the sensitivity curves relative to normalized frequency and normalized damping, and thus the frequency and damping insensitivities are independent of ω_{model}. Because the residual vibration $V(\cdot)$ cannot be written as a function of $\zeta_{norm} = \zeta/\zeta_{model}$, $V(\cdot)$ is dependent on ζ_{model}. Hence, the frequency, damping, and total insensitivities are dependent on ζ_{model}, and we shall present our results as plots of these quantities vs ζ_{model}.

Figure 4 shows the 5% frequency insensitivities I_f of the positive impulse single-mode ZV, ZVD, ZVDD, EI, and two-hump EI shapers for modeled damping constants varying from 0 to 0.2. As expected, the ZVDD has greater frequency insensitivities than the ZVD, which in turn has greater frequency insensitivity than the ZV shaping method. Similarly, the EI method is more sensitive to frequency modeling errors than the two-hump EI. The EI and ZVD positive impulse shapers each have three impulses, and, hence, given Eq. (3), the EI and ZVD shaper lengths are equal. Similarly, the two-hump EI and ZVDD shapers each have four impulses and, thus, are of the same length. However, as indicated in Fig. 4 and in the preceding section in Fig. 2, the EI and two-hump EI designs are more insensitive to frequency modeling errors than the equivalent-length ZVD and ZVDD shapers.

As anticipated from the preceding section, the damping insensitivities of the EI and two-hump EI designs are smaller than those for the equivalent-length ZVD and ZVDD designs (Fig. 5). In fact,

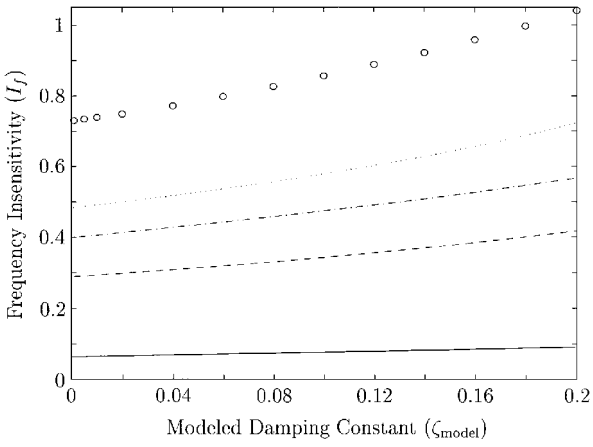

Fig. 4 Plot of the frequency insensitivity I_f as a function of modeled damping constant for various input shaper designs: ——, ZV; - - - -, ZVD; · · · · ·, ZVDD; – · –, EI; and ∘, two-hump EI.

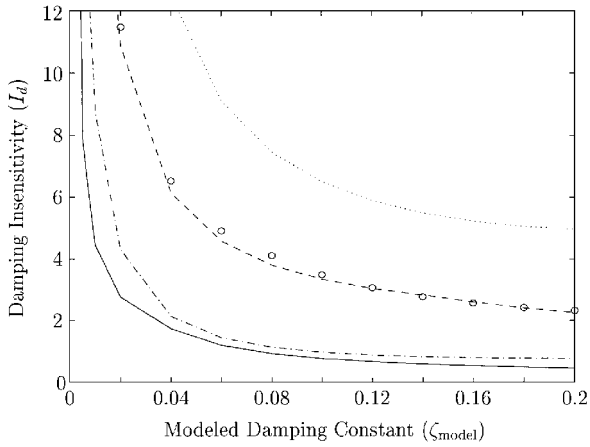

Fig. 5 Plot of the damping insensitivity I_d as a function of modeled damping constant for various input shaper designs: ——, ZV; - - - -, ZVD; · · · · ·, ZVDD; – · –, EI; and ∘, two-hump EI.

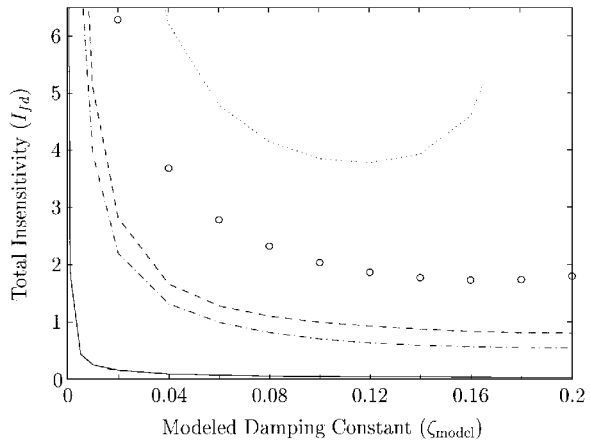

Fig. 6 Plot of the total insensitivity I_{fd} as a function of modeled damping constant for various input shaper designs: ——, ZV; - - - -, ZVD; · · · · ·, ZVDD; – · –, EI; and ∘, two-hump EI.

the damping insensitivity of the EI shaper is comparable to that for the nonrobust ZV shaper, and the damping insensitivity of the two-hump EI is almost exactly the same as that for the shorter-length ZVD shaper.

Comparing the total insensitivities of the various shapers in Fig. 6, we see that the derivative method (ZVD, ZVDD) of increasing robustness to modeling errors leads to greater total insensitivities than the extra insensitive methods (EI, two-hump EI) for the equivalent shaper lengths. That is, the ZVD gives greater total insensitivities than the EI method, and the ZVDD yields significantly larger total insensitivities than the two-hump EI.

The 5% total sensitivity contours for the ZV, ZVD, and ZVDD are generally convex; however, as the modeled damping constant gets larger, the contours can become concave. Figure 7 shows the 5% sensitivity contours for selected damping values for the ZV, ZVD, and ZVDD designs; the areas within the contours are the 5% total insensitivities I_{fd}. Because the axes are the normalized damping and frequency, the (1,1) location in each of the plots (denoted by a large dot) indicates the point where there is no modeling error. Note that, for smaller modeled damping constants, the contours run into the $\zeta = 0$ axis; ζ is required to be greater than or equal to zero for a dissipative flexible system. Whenever the contours run into the $\zeta = 0$ axis, the total insensitivity is computed as the area enclosed using the segment of the $\zeta = 0$ axis to close the contour. The 5% total sensitivity contours for the EI and two-hump EI methods are irregular and concave, as seen in Fig. 7.

IV. Discussion

From our analysis of the frequency and damping insensitivities of the various shaper types, we see that the EI and two-hump EI shapers give up some damping insensitivity to achieve increased frequency insensitivity over the ZVD and ZVDD methods. However, the total insensitivity results show that the derivative methods of increasing robustness (ZVD and ZVDD) lead to greater total insensitivities than the EI methods (EI and two-hump EI). This could be interpreted as the EI and two-hump EI methods giving up more damping insensitivity than the frequency insensitivity they gain.

In general, however, the results indicate that all of the shaper types considered have greater damping insensitivities than frequency insensitivities. This insensitivity to errors in modeled damping has been pointed out in Ref. 3 for the ZV, ZVD, and ZVDD methods. The EI and two-hump EI methods also show greater damping insensitivities than frequency insensitivities. If the modeling of the damping constants of the flexible modes of a system is accurate and there are only small uncertainties in the damping, then the EI (EI and multihump EI) methods would be appropriate for accurate control of the flexible system. However, in many systems, damping is often more difficult to model accurately than the modal frequencies, and the derivative methods (ZVD, ZVDD, etc.) may be more appropriate.

There are always uncertainties in the modeling of both frequency and damping, and it is important to address both in the input shaping design. Given the uncertainties in frequency and damping, the input shaping design used should yield a contour plot at the acceptable vibration level in ζ–ω space that encompasses the entire uncertainty region. Often, the uncertainties in modeled frequency and damping are expressed in the form

$$\omega_{\mathrm{lo}_j} \le \omega_j \le \omega_{\mathrm{hi}_j}, \qquad \zeta_{\mathrm{lo}_j} \le \zeta_j \le \zeta_{\mathrm{hi}_j}, \qquad j = 1, \ldots, n \tag{5}$$

In normalized form for a one-mode system, we would have

$$\frac{\omega_{\mathrm{lo}}}{\omega_{\mathrm{model}}} \le 1 \le \frac{\omega_{\mathrm{hi}}}{\omega_{\mathrm{model}}}, \qquad \frac{\zeta_{\mathrm{lo}}}{\zeta_{\mathrm{model}}} \le 1 \le \frac{\zeta_{\mathrm{hi}}}{\zeta_{\mathrm{model}}} \tag{6}$$

It is clear that, for each mode, the uncertainty leads to a rectangle in ζ–ω space, a shape very different from the contours in Fig. 7.

For uncertainties expressed in this manner, it is of interest to know whether an input shaping design can guarantee vibration levels below the acceptable vibration level V_a for the entire range of uncertainty. This requires the contour at V_a in ζ–ω space to encompass the uncertainty region. From our analysis of one-mode systems, we have an approximate idea of the sizes and shapes of the 5% sensitivity contours from Figs. 4–7. Given a standard uncertainty form of Eq. (6), however, it is still difficult to judge whether a particular positive shaper design's 5% sensitivity contour encompasses the entire uncertainty region without evaluating the sensitivity surface over the uncertainty region.

We have computed curve fit formulas for a number of quantities that define the 5% sensitivity contours as functions of ζ_{model}. Because the contours for the ZV, ZVD, and ZVDD shapers are of

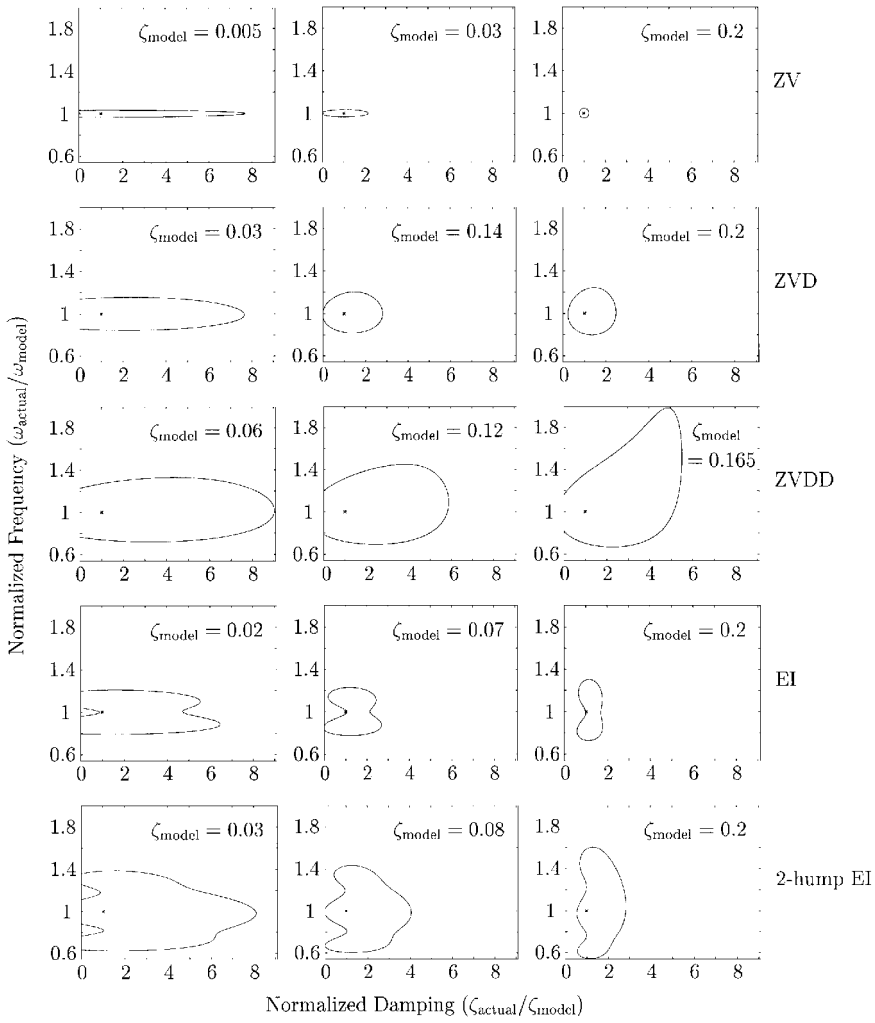

Fig. 7 Shapes of the 5% total sensitivity contours for various modeled damping values and shaper designs.

similar shapes, similar quantities and formulas are used to approximate these contours. The important quantities are labeled for a ZVD contour in Fig. 8. The offset is the normalized damping axis coordinate of the centroid of the region enclosed by the contour. If offset is 1, then the contour region is centered about ζ_{model}. Generally, the input shapers are more tolerant for larger dampings than smaller dampings, and so the offset parameter tends to be greater than 1. The parameters ω_{min} and ω_{max} are the minimum and maximum normalized frequencies on the contour when the normalized damping is set to the offset value. For the ZV, ZVD, and ZVDD shapers, the contours are approximately symmetric about the $\omega_{actual}/\omega_{model} = 1$ axis. The upper half and lower half are approximately parabolas, and we can define two parameters c_1 and c_2, which along with ω_{min} and ω_{max} can approximate the shapes of these halves:

$$\omega_{norm_{lower\_half}} \approx \omega_{min} + c_1|\zeta_{norm} - \text{offset}| + c_2|\zeta_{norm} - \text{offset}|^2$$

$$\omega_{norm_{upper\_half}} \approx \omega_{max} - c_1|\zeta_{norm} - \text{offset}| - c_2|\zeta_{norm} - \text{offset}|^2$$

where for a range of normalized damping ratios ζ_{norm} about the offset value, the corresponding normalized frequencies that comprise the sensitivity contour can be computed by the preceding formulas. We have computed curve fit formulas for the offset, ω_{min}, ω_{max}, c_1, and c_2 as a function of ζ_{model} for $0 \le \zeta_{model} \le 0.2$ for the ZV and ZVD positive shapers and for $0 \le \zeta_{model} \le 0.14$ for the ZVDD. The formulas are given in Table 1 and are accurate to within 5% over these ranges. They tend to be less accurate for lower damping constants because of the rapid change in contour size in this range (as indicated in Fig. 6). More accurate formulas, if desired, can be obtained if we restrict ourselves to smaller ranges of ζ_{model}.

For the EI and two-hump EI shapers, the sensitivity contours are more complex in shape. However, for simplicity, we have also approximated the upper and lower halves of the contours with parabolas. For the EI shaper, the sensitivity contour has a neck, and so it is important to know the width of the neck to be able to determine whether the contour encompasses an uncertainty region of the form of Eq. (6). The parameter determining the lower damping side of the neck (see Fig. 8), D_{min}, is always equal to 1. This is because the EI shapers are designed so that there is 5% (or V_a) residual vibration at the modeling frequency and modeling damping. [See Fig. 2; the EI and multihump EI shapers could be designed such that the humps have a maximum residual vibration level less than 5% (or less than V_a). This would reduce the frequency insensitivity and increase the damping insensitivity levels compared to those shown for the EI-type shapers in Figs. 4 and 5. As the maximum residual vibration level of the hump(s) is decreased, the EI and multihump EI shaper designs approach the ZVD and multiderivative shaper designs.] The higher damping side of the neck, D_{max}, varies with ζ_{model}. Curve fit formulas for the offset, ω_{min}, ω_{max}, c_1, c_2, and D_{max} as a function of ζ_{model} for $0 \le \zeta_{model} \le 0.2$ for the EI positive shaper are given in Table 1.

For the two-hump EI shaper, there are indentations in the contour on the lower damping side (Fig. 7). As with the EI shaper, because the two-hump shaper is designed so that the humps have a maximum of 5% residual vibration (see Fig. 2 and parenthetical notation in preceding paragraph), the parameter D_{min} in the bottom plot in Fig. 8 is always equal to 1. Curve fit formulas for the offset, ω_{min}, ω_{max}, c_1, and c_2 as functions of ζ_{model} for $0 \le \zeta_{model} \le 0.2$ for the two-hump EI positive shaper are given in Table 1. The formulas for the EI and two-hump EI shapers are accurate to within 10%. More accurate formulas can be obtained if we restrict ourselves to smaller ranges of ζ_{model} as well as use a more complicated curve than a parabola to fit the upper and lower halves of the EI and two-hump EI sensitivity contours.

Table 1 Formulas for determining whether various shaper designs can guarantee less than 5% residual vibration over the uncertainty region of Eq. (6)

Shaper	Curve fit formulas
ZV	$\text{offset} = 2.0771\exp(-278.5415\zeta_{\text{model}}) + 1.0276$
	$\omega_{\min} = 0.9691 - 0.0463\zeta_{\text{model}} - 0.0875\zeta_{\text{model}}^2$
	$\omega_{\max} = 1.0309 + 0.0484\zeta_{\text{model}} + 0.1093\zeta_{\text{model}}^2$
	$c_1 = -0.0223\zeta_{\text{model}} + 0.5805\zeta_{\text{model}}^2$
	$c_2 = 0.1346\zeta_{\text{model}} + 22.2562\zeta_{\text{model}}^2 - 12.9057\zeta_{\text{model}}^3$
ZVD	$\text{offset} = 46.4681\exp(-269.4522\zeta_{\text{model}}) + 1.4500$
	$\omega_{\min} = 0.8622 - 0.1959\zeta_{\text{model}} - 0.3875\zeta_{\text{model}}^2$
	$\omega_{\max} = 1.1367 + 0.2325\zeta_{\text{model}} + 1.1239\zeta_{\text{model}}^2$
	$c_1 = 0.0376\zeta_{\text{model}} - 0.0616\zeta_{\text{model}}^2$
	$c_2 = 0.0094\zeta_{\text{model}} + 5.5328\zeta_{\text{model}}^2 - 5.5508\zeta_{\text{model}}^3$
ZVDD	$\text{offset} = 174.8072\exp(-223.8919\zeta_{\text{model}}) + 2.7000$
	$\omega_{\min} = 0.7515 - 0.3132\zeta_{\text{model}} - 0.4350\zeta_{\text{model}}^2$
	$\omega_{\max} = 1.2648 + 0.1694\zeta_{\text{model}} + 9.9607\zeta_{\text{model}}^2$
	$c_1 = -0.0136\zeta_{\text{model}} + 0.2332\zeta_{\text{model}}^2$
	$c_2 = 4.7531\zeta_{\text{model}}^2 - 15.3142\zeta_{\text{model}}^3$
EI	$\text{offset} = 1212.2\exp(-4840.9\zeta_{\text{model}}) + 1.3500$
	$\omega_{\min} = 0.8009 - 0.2359\zeta_{\text{model}} - 0.3648\zeta_{\text{model}}^2$
	$\omega_{\max} = 1.2000 + 0.2207\zeta_{\text{model}} + 1.0978\zeta_{\text{model}}^2$
	$c_1 = 0.5086\zeta_{\text{model}} + 0.7022\zeta_{\text{model}}^2$
	$c_2 = 15.2649\zeta_{\text{model}}^2 + 2.1945\zeta_{\text{model}}^3$
	$D_{\min} = 1$
	$D_{\max} = 76.2438\exp(-167.53\zeta_{\text{model}}) + 1.8000$
Two-hump EI	$\text{offset} = 943.9863\exp(-5571.4\zeta_{\text{model}}) + 1.3500$
	$\omega_{\min} = 0.6392 - 0.3837\zeta_{\text{model}} - 0.4384\zeta_{\text{model}}^2$
	$\omega_{\max} = 1.3646 + 0.5733\zeta_{\text{model}} + 2.9571\zeta_{\text{model}}^2$
	$c_1 = 0.0756\zeta_{\text{model}} - 0.0611\zeta_{\text{model}}^2$
	$c_2 = 0.3520\zeta_{\text{model}} + 3.6050\zeta_{\text{model}}^2 - 6.9081\zeta_{\text{model}}^3$
	$D_{\min} = 1$

Using the formulas in Table 1 and the following procedure, we can easily determine whether the 5% sensitivity contour of the various shapers covers an uncertainty of the form (6).

1) Given the type of shaper (ZV, ZVD, ZVDD, EI, or two-hump EI), ζ_{model}, and Eq. (6), let

$$\zeta_l = \frac{\zeta_{\text{lo}}}{\zeta_{\text{model}}}, \qquad \zeta_h = \frac{\zeta_{\text{hi}}}{\zeta_{\text{model}}}, \qquad \omega_l = \frac{\omega_{\text{lo}}}{\omega_{\text{model}}}, \qquad \omega_h = \frac{\omega_{\text{hi}}}{\omega_{\text{model}}}$$

2) For the given ζ_{model}, compute the offset, $\omega_{\min}$, $\omega_{\max}$, c_1, c_2, and $D_{\max}$ from Table 1. For the ZV, ZVD, and ZVDD shapers, set $D_{\min} = 0$ because there is no indentation in the sensitivity contour on the low damping side (Fig. 8); for the ZV, ZVD, ZVDD, and two-hump EI shapers, set $D_{\max} = +\infty$ because there is no indentation on the high damping side (Fig. 8). If any of

$$\zeta_l < D_{\min}, \qquad \zeta_h > D_{\max}, \qquad \omega_l < \omega_{\min}, \qquad \omega_h > \omega_{\max}$$

hold, then the uncertainty region is not encompassed by the 5% sensitivity contour, and the next step should be skipped.

3) For the given uncertainty in damping, ζ_l and ζ_h, let us compute the largest range of frequency uncertainty $[\omega_{\text{lo\_bound}}, \omega_{\text{hi\_bound}}]$ that can be accommodated. Let

$$\Delta_p = \max(\zeta_h - \text{offset}, 0), \qquad \Delta_n = \text{offset} - \zeta_l$$

and

$$\Delta = \max(\Delta_p, \Delta_n)$$

Because the ζ_l and ζ_h values may be asymmetric about the offset parameter, the larger of Δ_p and Δ_n is used because it will be the limiting factor in whether the uncertainty region is encompassed by the sensitivity contour. We can now compute the bounds on the normalized frequency such that the rectangular region described by ζ_l, ζ_h, $\omega_{\text{lo\_bound}}$, and $\omega_{\text{hi\_bound}}$ is encompassed by the 5% sensitivity contour:

$$\omega_{\text{lo\_bound}} = \omega_{\min} + c_1\Delta + c_2\Delta^2$$

$$\omega_{\text{hi\_bound}} = \omega_{\max} - c_1\Delta - c_2\Delta^2$$

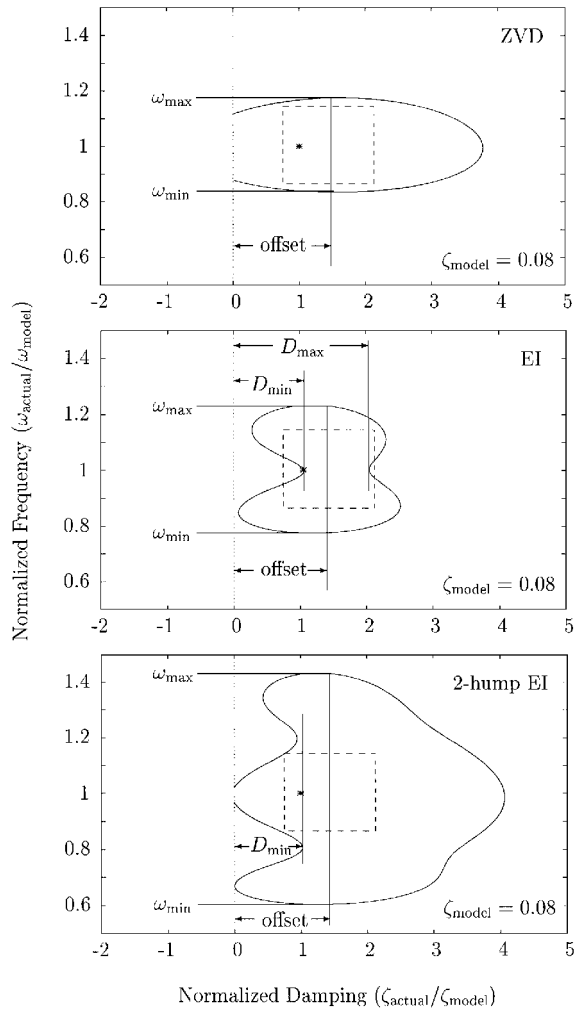

Fig. 8 Parameters used to approximate the shapes of the sensitivity contours for various shaper designs.

Now, if

$$\omega_l < \omega_{\text{lo\_bound}} \qquad \text{or} \qquad \omega_h > \omega_{\text{hi\_bound}}$$

then the uncertainty region is not encompassed by the 5% sensitivity contour. Otherwise, the uncertainty region is encompassed by the 5% sensitivity contour.

This procedure provides a quick way to determine whether a shaper sensitivity contour encompasses a rectangular uncertainty region as in Eq. (6) without having to compute the entire sensitivity surface in ζ–ω space.

Example: To illustrate the procedure, suppose that, in the modeling of a one-mode flexible system, we determine that

$$30 \text{ rad/s} \le \omega_{\text{actual}} \le 39.7 \text{ rad/s} \tag{7}$$

$$0.06 \le \zeta_{\text{actual}} \le 0.17 \tag{8}$$

Let us choose

$$\omega_{\text{model}} = 34.7 \qquad \text{and} \qquad \zeta_{\text{model}} = 0.08 \tag{9}$$

For the ZVD shaper, we have the following data.

1) From the model and uncertainty information, we have

$$\zeta_l = 0.75, \qquad \zeta_h = 2.125, \qquad \omega_l = 0.8646, \qquad \omega_h = 1.1441$$

2) From the formulas for the ZVD shaper in Table 1, we have

$$\text{offset} = 1.4500, \qquad \omega_{\min} = 0.8440, \qquad \omega_{\max} = 1.1625$$

$$c_1 = 0.002614, \qquad c_2 = 0.03332$$

$$D_{\min} = 0, \qquad D_{\max} = +\infty$$

Because $\zeta_l > D_{\min}$, $\zeta_h < D_{\max}$, $\omega_l > \omega_{\min}$, and $\omega_h < \omega_{\max}$, we need to proceed to step 3 to determine whether the uncertainty region is encompassed by the 5% ZVD sensitivity contour.

3) We compute

$$\Delta_p = 0.675, \qquad \Delta_n = 0.7, \qquad \text{and} \qquad \Delta = 0.7$$

and

$$\omega_{\text{lo\_bound}} = 0.8622 \qquad \text{and} \qquad \omega_{\text{hi\_bound}} = 1.1443$$

Now, because $\omega_l > \omega_{\text{lo\_bound}}$ and $\omega_h < \omega_{\text{hi\_bound}}$, the uncertainty region is encompassed by the 5% ZVD sensitivity contour.

The 5% ZVD contour for this example, i.e., for $\zeta_{\text{model}} = 0.08$, is shown in the upper plot in Fig. 8, with the rectangular uncertainty region of the example shown completely within the contour. We can follow the same procedure for determining whether the other shaper types (ZV, ZVDD, EI, and two-hump EI) also encompass the uncertainty region in the preceding example, and we will find that the only other shaper that can handle this uncertainty is the ZVDD. The EI and the two-hump EI fail because they are not robust to damping errors below ζ_{model} as embodied in the $D_{\min}$ parameters and shown in Fig. 8. [The two-hump EI contour does not encompass the large-ω/small-ζ corner of the uncertainty region. Because the procedure does not allow any damping uncertainty below ζ_{model} for the two-hump EI, the procedure tends to give conservative answers for the two-hump EI when there is very little uncertainty in the modeling frequency; that is, if $\omega_l > 0.9$ and $\omega_h < 1.1$, the two-hump EI can tolerate some damping uncertainty below ζ_{model} (Figs. 7 and 8); however, the outlined procedure will conclude that the two-hump EI does not encompass any rectangular uncertainty with $\zeta_l < 1$. For small frequency uncertainties, it is overkill to use the two-hump EI shaper; for larger frequency uncertainties where the two-hump EI is to be considered, the 5% contour can encompass rectangular uncertainties of Eq. (6) only if there is no damping uncertainty below ζ_{model}.] If the lower bound on ζ_{actual} in Eq. (8) is 0.08 and the model is still chosen as in Eq. (9), then the ZVD, ZVDD, and two-hump EI 5% sensitivity contours encompass the uncertainty region. If the upper bound on the damping uncertainty in Eq. (8) is also lowered to 0.144, then the EI sensitivity contour will encompass the uncertainty region.

Because the total sensitivity contours are functions of ζ_{model}, the selection of a particular model damping ratio within the uncertainty range is important. It is difficult to know exactly how to choose ζ_{model} such that the total sensitivity contour is more likely to encompass the uncertainty region, but the described procedure allows several choices of ζ_{model} to be quickly evaluated rather than computing the sensitivity surfaces and resulting contours for each ζ_{model} considered.

V. Conclusions

We have defined a damping insensitivity measure that indicates how robust an input shaper design is to modeling uncertainty in damping, and we have further defined a total insensitivity measure that addresses modeling uncertainty in both frequencies and damping constants of flexible systems. Using these measures, along with an earlier defined frequency insensitivity measure, we have analyzed several input shaping designs, and the results show that EI and two-hump EI input shapers, which have previously been shown to have larger frequency insensitivities, have smaller damping insensitivities and smaller total insensitivities compared to equal-length ZVD and ZVDD shapers.

All of the shaper types considered have greater damping insensitivities than frequency insensitivities, and whether the larger damping and total insensitivities of the ZVD and ZVDD methods are needed or the larger frequency insensitivities of the EI and two-hump EI are needed depends on the estimated accuracy of the modeling with respect to the frequency and damping parameters. We have presented the shapes of the 5% sensitivity contours of the various shaper designs in normalized ζ–ω space. Given the uncertainties in frequency and damping, the input shaping design used should yield a contour plot at the acceptable vibration level in ζ–ω space that encompasses the entire uncertainty region. Using curve fit formulas to approximate the sensitivity contours, we have also outlined a quick and useful way for determining whether an input shaper can handle a common form of frequency and damping uncertainty without needing to compute the entire sensitivity surface.

Acknowledgments

The author gratefully acknowledges support for this work under a National Science Foundation Early Faculty CAREER Development Award (Grant CMS-9625086) and an Office of Naval Research Young Investigator Award.

References

[1] Book, W. J., "Controlled Motion in an Elastic World," *Journal of Dynamic Systems, Measurement and Control*, Vol. 115, No. 2, 1993, pp. 252–261.

[2] Junkins, J. L., and Kim, Y., *Introduction to Dynamics and Control of Flexible Structures*, AIAA Education Series, AIAA, Washington, DC, 1993.

[3] Singer, N., and Seering, W., "Preshaping Command Inputs to Reduce System Vibration," *Journal of Dynamic Systems, Measurement and Control*, Vol. 112, No. 1, 1990, pp. 76–82.

[4] Singh, T., and Vadali, S. R., "Robust Time-Optimal Control: A Frequency Domain Approach," *Journal of Guidance, Control, and Dynamics*, Vol. 17, No. 2, 1994, pp. 346–353.

[5] Singhose, W., Seering, W., and Singer, N., "Residual Vibration Reduction Using Vector Diagrams to Generate Shaped Inputs," *Journal of Mechanical Design*, Vol. 116, No. 2, 1994, pp. 654–659.

[6] Wie, B., Sinha, R., and Liu, Q., "Robust Time-Optimal Control of Uncertain Structural Dynamic Systems," *Journal of Guidance, Control, and Dynamics*, Vol. 16, No. 5, 1993, pp. 980–983.

[7] Rappole, B. W., Singer, N. C., and Seering, W. P., "Multiple-Mode Input Shaping Sequences for Reducing Residual Vibrations," *Proceedings of the ASME Mechanisms Conference* (Minneapolis, MN), Vol. DE–71, American Society of Mechanical Engineers, New York, 1994, pp. 11–16.

[8] Singhose, W., Seering, W., and Singer, N., "The Effect of Input Shaping on Coordinate Measuring Machine Repeatability," *Proceedings of the IFToMM World Congress on the Theory of Machines and Mechanisms* (Milan, Italy), Vol. 4, Elsevier Science, Oxford, England, UK, 1995, pp. 2930–2934.

[9] Tuttle, T. D., and Seering, W. P., "Vibration Reduction in Flexible Space Structures Using Input Shaping on MACE: Mission Results," *Proceedings of the IFAC World Congress* (San Francisco, CA), Vol. D (Control Design II, Optimization), Elsevier Science, Oxford, England, UK, 1996, pp. 55–60.

[10] Jansen, J. F., "Control and Analysis of a Single-Link Flexible Beam with Experimental Verification," Oak Ridge National Lab., Rept. ORNL/TM-12198, Oak Ridge, TN, 1992.

[11] Magee, D. P., and Book, W., "Filtering Micro-Manipulator Wrist Commands to Prevent Flexible Base Motion," *Proceedings of the American Control Conference* (Seattle, WA), Inst. of Electrical and Electronics Engineers, Piscataway, NJ, 1995, pp. 924–928.

[12] Singhose, W., Derezinski, S., and Singer, N., "Extra-Insensitive Shapers for Controlling Flexible Spacecraft," *Proceedings of the AIAA Guidance, Navigation, and Control Conference* (Scottsdale, AZ), AIAA, Washington, DC, 1994, pp. 1122–1130.

[13] Singhose, W., Porter, L., and Singer, N., "Vibration Reduction Using Multi-Hump Extra-Insensitive Input Shapers," *Proceedings of the American Control Conference* (Seattle, WA), Inst. of Electrical and Electronics Engineers, Piscataway, NJ, 1995, pp. 3830–3834.

[14] Pao, L. Y., and Singhose, W. E., "Unity Magnitude Input Shapers and Their Relation to Time-Optimal Control," *Proceedings of the IFAC World Congress* (San Francisco, CA), Vol. A (Robotics, Components, and Instruments), Elsevier Science, Oxford, England, UK, 1996, pp. 385–390.

[15] Singhose, W., Singer, N., and Seering, W., "Design and Implementation of Time-Optimal Negative Input Shapers," *Proceedings of the ASME International Mechanical Engineering Congress and Exposition* (Chicago, IL), Vol. DSC 55–1, American Society of Mechanical Engineers, New York, 1994, pp. 151–157.

[16] Pao, L. Y., and Singhose, W. E., "A Comparison of Constant and Variable Amplitude Command Shaping Techniques for Vibration Reduction," *Proceedings of the IEEE Conference on Control Applications* (Albany, NY), Inst. of Electrical and Electronics Engineers, Piscataway, NJ, 1995, pp. 875–881.

[17] Bhat, S. P., and Miu, D. K., "Solutions to Point-to-Point Control Problems Using Laplace Transform Technique," *Journal of Dynamic Systems, Measurement and Control*, Vol. 113, No. 3, 1991, pp. 425–431.

[18] Pao, L. Y., and Singhose, W. E., "On the Equivalence of Minimum Time Input Shaping with Traditional Time-Optimal Control," *Proceedings of the IEEE Conference on Control Applications* (Albany, NY), Inst. of Electrical and Electronics Engineers, Piscataway, NJ, 1995, pp. 1120–1125.

[19] Singh, T., and Heppler, G. R., "Shaped Input Control of a System with Multiple Modes," *Journal of Dynamic Systems, Measurement and Control*, Vol. 115, No. 3, 1993, pp. 341–347.

[20] Tuttle, T. D., and Seering, W. P., "A Zero-Placement Technique for Designing Shaped Inputs to Suppress Multiple-Mode Vibration," *Proceedings of the American Control Conference* (Baltimore, MD), Inst. of Electrical and Electronics Engineers, Piscataway, NJ, 1994, pp. 2533–2537.